JOURNAL OF AIRCRAFT
Vol. 41, No. 6, November–December 2004

Model of the Neuromuscular Dynamics of the Human Pilot's Arm

M. M. (René) van Paassen,* J. C. (Hans) van der Vaart,† and J. A. (Bob) Mulder‡
Delft University of Technology, 2629 HS Delft, The Netherlands

This paper presents a model for the neuromuscular system of the pilot's arm. The model was developed in order to gain a better understanding of the interaction between a side stick and the human arm. In the model, the dynamics of the neuromuscular system and of the stick are considered separately, and so control situations where the stick and arm are subjected to accelerations (in a moving vehicle) or where haptic feedback is applied through the stick can be studied. Two of the experiments to provide parameter values for the model are described. One experiment is intended for determination of the parameters of the neuromuscular systems hardware, and the other for determining the control of this hardware.

Nomenclature

B_c	=	damping constant of the skin
B_m	=	damping constant of the muscle
I_a	=	moment of inertia of the arm
K_c	=	elasticity constant of the skin
K_e	=	series elasticity constant of the muscle
K_{pec}	=	parallel elasticity constant of the muscle
m_s	=	moment exerted by the pilot on the stick
m_{wl}	=	disturbing moment on limb
m_{ws}	=	disturbing moment on stick
q_m	=	muscle activation signal
u_p	=	pilot visual input, display presentation
x_l	=	limb position
x_s	=	stick (manipulator) position
x_t	=	intended limb position, control output of the pilot's equalization

Introduction

MANIPULATOR design and tuning is sometimes more of an art than a science. A prominent example of a case where the interaction between the manipulator and the pilot's arm was not foreseen is the General Dynamics F-16, in which the original design of the side-stick controller suffered from oversensitivity, which led to problems during high-speed taxi tests.[1] A following redesign suffered from roll-ratchet problems.[2]

By using a model of the neuromuscular system that enables an analysis of the interaction between the manipulator and the pilot's arm while subjected to accelerations, that is, in a moving vehicle, such cases could be analyzed beforehand. Other application areas for such a model are the analysis and design of so-called active manipulators (the active stick by[3] or the "Assistive Aidi" described in Ref. 4), in which an active servo element is used to provide feedback from the controlled system or from other sources such as threats in the environment.

Previous work on modeling the neuromuscular system is given in. Refs. 5, and 6. In these works the manipulator and neuromuscular system are lumped together in a single model, making them less suitable for studying interaction between these. Other studies on neuromuscular system models for describing manual control situations were based on theory about muscle and arm dynamics, such as, Refs. 7–9 or on the results from tests in which the whole body was subjected to acceleration.[10–12]

In this paper a model for the neuromuscular system derived from theory is validated with experiments with a control loaded side stick, in a fixed-base simulation. The model was elaborated for the case of roll control with a side stick. The model can be used for the analysis and design of active manipulators and offers an alternative method (i.e., not requiring whole-body acceleration tests) for analysis of biodynamic interference.

Model

Outline of the Model

The model is partly based on models of the neuromuscular system available in the literature. The muscle itself is modelled as a three-component Hill-type model.[13,14] This is combined with models for the skin flexibility and the limb inertia and a new model for the control of the neuromuscular system.

A distinction will be made between the hardware and the software or control parts of the model. The hardware parts model the physical, force-generating, or force-transferring parts of the neuromusculoskeletal system, such as the muscles, the bones, and the skin and connecting tissues. The combination of this hardware part and the manipulator is considered as a plant. Figure 1 shows the overall structure of the model. The output of the hardware plant is the stick position x_s. The input to the side stick is the moment m_s exerted by the pilot. The hardware submodel (muscle, skin, and limb) has as input the activation signal q_m, which controls muscle activity, and as a feedback signal the stick position x_s. The muscle activation signal q_m is provided as an output of the software submodel (control and correction). A feedback to this submodel is provided by the limb position x_l. The input to the software submodel is the pilot's intended stick position x_t, which is based on his observation of a certain variable to be controlled in the control task at hand. External disturbing moments m_{wl} and m_{ws} are acting on the muscle, skin and limb hardware and the side stick respectively.

This model supposes that control of the muscles themselves does not require conscious attention from the pilot. That task is performed by motor control centers in the brain and neural feedback loops at the spinal level. To reflect this in the model, the input to the neuromuscular system x_t is taken to be a target or reference position for the limb.

Sensors in the limb measure muscle length, muscle force, limb position, and pressure on the skin. The stick position as such is supposed not to be available as a feedback signal, unless the pilot is looking at the stick. In the model the limb position x_l will be used as the only feedback signal that is available to the software part of the model.

The properties of the neuromuscular system hardware are assumed to be invariant, and the fact that the model contains submodels for the neuromuscular hardware and software has the advantage that data on muscle models and limb inertia available in biophysics

Received 8 December 2000; revision received 6 November 2003; accepted for publication 10 November 2003.

*Assistant Professor, Faculty of Aerospace Engineering, Kluijverweg 1.
†Associate Professor, Faculty of Aerospace Engineering, Kluijverweg 1.
‡Full Professor, Faculty of Aerospace Engineering, Kluijverweg 1. Member AIAA.

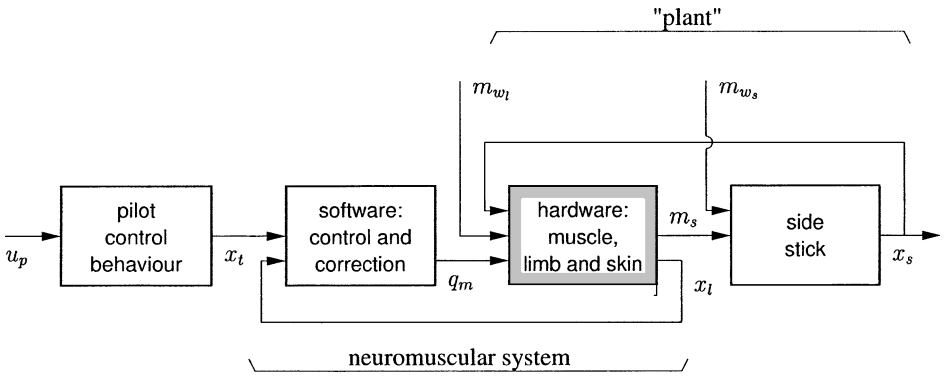

Fig. 1 Overview of the different components of the pilot and his neuromuscular system.

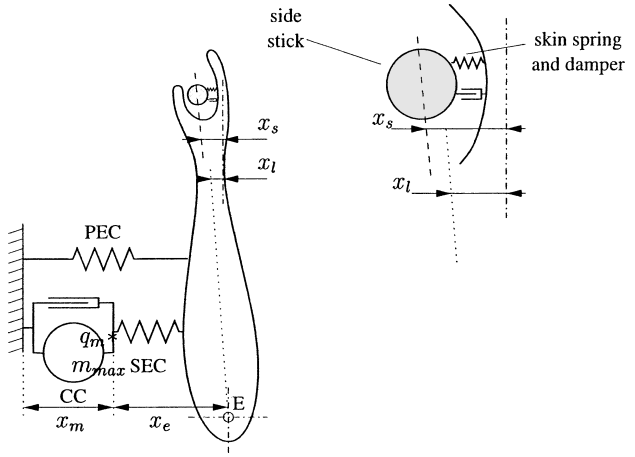

Fig. 2 Schematic top view of the pilot's arm showing the hardware of the neuromuscular system model; see the shaded box in Fig. 1.

literature[13] can be used as an initial estimate for model parameters. On the other hand humans are flexible in adjusting their control strategies[15] or strength of responses to disturbances[16] to the task and the manipulator at hand. In the model these adaptations remain restricted to the software part of the model.

Neuromuscular System Hardware

To keep the model simple, a number of assumptions were made. The first assumption concerns the manner in which the pilot moves the side stick in a roll control task. It is assumed that in moving the stick he or she keeps the wrist joint stiff, keeps the elbow in a fixed location, and rotates the lower arm sideways to move the stick. This allows the modeling of the limb's mass with a single moment of inertia. This assumption is consistent with visual observations of subjects manipulating the side stick. It is also assumed that the trunk of the pilot remains fixed relative to the airframe.

The hardware part of the muscle model, as contained in the shaded box of Fig. 1, is illustrated in Fig. 2. The limb's inertia is represented by one rigid body that can rotate about an imaginary vertical axis through the elbow.

Complex muscle groups linking the trunk, shoulder blade, and upper arm control the inward and outward rotation of the upper arm and lower arm. The action of these muscle groups is represented by a single, linear, muscle model, that has both a pulling and pushing action. The model links the limb with the rigid trunk and is a so-called three-component or Hill-type muscle model.[13,14] The muscle model contains a parallel elastic component, which models the elastic properties of a passive, inactive muscle, a contractile component (CC), which is the active element of the muscle model, consisting of a force generator in parallel with a damper. The force from the CC is passed to the limb by a third element, the series elastic element (SEC), modeled by a relatively stiff spring. Originally, a pair of nonlinear models was considered. However, the data from the experiments did not allow the identification of the parameters of this model,[17] and considering the limited range of exerted forces and moments a linear approximation for the nonlinear properties of the limb should result in a sufficiently accurate model.

Early in the development of the model for the neuromuscular system, experiments were done in which test inputs, consisting of changes in stick position, were applied to a subject's arm.[18,19] From these experiments it was found that a flexible element had to be introduced between the limb mass and the side stick. This element, called the skin model, represents the flexibility and the damping in tissues between the limb and the side stick handle, modeled by a spring and a damper mounted in parallel, between the limb rigid body and the side stick.

For ease of calculation, the position of the limb and stick and the various muscle lengths or positions internally in the model will be expressed as rotations of the lower arm around the vertical axis through the elbow rotation point. Likewise, forces on the stick have been rescaled to moments around this point. This also causes the model parameter values to be independent of the particular dimensions of the stick.

Neuromuscular System Software

For the present model it is assumed that an internal representation of the plant, that is, the neuromuscular system hardware and the side stick, is used by the pilot to generate control signals for the muscles. The application of the internal representation enables the model to produce the fast, ballistic-type, movements that are also observed in humans, and it also agrees with findings from literature.[15,20]

In the model the internal representation is assumed to be a correct copy of the model for the neuromuscular hardware and the side stick; this copy will be called the internal model. The control signal for the muscle model q_f is generated by embedding this internal model in a closed control loop (see Fig. 3). The input of this loop is the target position for the limb x_t. The difference between the target position and the limb position of the internal representation x_{l_i} is filtered to obtain q_f.

Adjustment of the parameters of an internal model filter modifies the response of the neuromuscular system to the commanded target position for the limb x_t; such adjustments can for example be varied to let the model generate either smooth or more aggressive movements. Adjustment of the filter can also be necessary to compensate for different stick and task properties.

Although there is evidence that an internal representation is used in the neuromuscular system to generate control signals for the muscles, it is also clear that there are various control loops to correct for disturbances on the limb.[15] Reflexes are the effect of these control loops. To simulate this with the model, a neural feedback loop was added, represented with q_n in Fig. 3.

In the real neuromuscular system, a number of sensors provide information about the muscles and the limb and can thus be seen as a potential basis for the feedback loops in the neuromuscular system. Examples are Golgi tendon organs, which respond to force

in the tendons, muscle spindles, which respond to muscle length and extension velocity, and joint sensors, which give a response at certain joint angles. However, the knowledge that is presently available about these components and their connections is insufficient to allow a detailed modeling of the feedback, and the resulting model would become too complicated for our purpose. It is therefore necessary to resort to concepts of control theory to represent the neural feedback, and a single lead-lag filter with a time delay is used in the model.

To let both the open-loop behavior on the basis of the internal model and the closed-loop reactions to disturbances coexist in the model, the input of the neural feedback filter (Fig. 3) is not based on the target position, but on the difference between the limb position given by the hardware part of the model, and the limb position predicted by the internal model ($x_l - x_{l_i}$). The output is a corrective muscle activation q_n, which is added to the signal calculated with the internal model, to form the total control signal for the muscle q_m.

With this architecture of the model, the filter for the internal model and the internal model itself completely define the model's response to the commanded limb position x_t, while the neuromuscular system hardware, stick properties, and feedback filter define the model's response to disturbances on the stick and limb.

To describe a manual control situation, as present in experiment 2, the model is combined with a model for the pilot's control behavior. The model by McRuer and Jex[5] is used for this purpose. Usually this model is used to describe the pilot including his neuromuscular system and the manipulator. In the present case the output of this model is the target position for the limb x_t and thus the input signal for the model of the neuromuscular system. The input of the model for the pilot's control behavior (u_p) is the error perceived on the display.

The equations describing the software part of the model are given in Table 1.

Table 1 Equations describing the software part of the neuromuscular system model

Description	Transfer function
Pilot control behavior Input: pilot visual input u_p Output: neuromuscular system target position x_t	$H_p(s) = K_p \dfrac{1+\tau_{p_L} s}{1+\tau_{p_l} s} e^{-\Delta t_p s}$
Internal model equalization filter Input: $x_t - x_{l_i}$ Output: q_f	$H_f(s) = K_f \dfrac{1+\tau_{f_L} s}{1+\tau_{f_l} s}$
Neural feedback Input: $x_{l_i} - x_l$ Output: q_n	$H_n(s) = K_n \dfrac{1+\tau_{n_L} s}{1+\tau_{n_l} s} e^{-\Delta t_n s}$
Neural activation internal muscle model	$q_{m_i} = q_f$
Neural activation external muscle model	$q_m = q_f + q_n$

Experiment I: Hardware

Experiment Principle

Experiment 1 is intended to estimate the parameters of the hardware part of the neuromuscular model. These are the parameters for the skin flexibility model (damping and elasticity component B_c and K_c), the limb moment of inertia I_l, the parallel elastic component elasticity K_{pec}, the series elastic component elasticity K_e, and the contractile component damping B_m. The maximum moment generated in the contractile component $m_{\max}$ is assumed fixed, at a value of 40 Nm, as this parameter only serves as a scaling factor for the muscle activation signal q_m.

The hardware part of the neuromuscular system can be viewed as a system with two inputs q_m and x_s and one output, the moment generated on the side stick m_s. In the experiment the side-stick position x_s was used as test input. This was easily done with the side stick used in the experiments, which was coupled to a hydraulic motor.

The other input signal for the neuromuscular system hardware, the muscle activation q_m, ideally should have remained constant in this experiment. To ensure the subjects' cooperation here, an error measure indicating change in muscle activation input was presented on the display. This measure was calculated on the basis of Smoothed, Rectified ElectroMyography (SRE) signals measured from the subject's muscles and processed to indicate changes in the levels of these signals. Similar smoothed and subsequently rectified electromyography (EMG) signals (SRE) have been identified as an indicator for muscle activation.[14,21,22]

A small bar on a visual display in front of the subject would move upwards when changes in the SRE levels were detected. In a number of training sessions the subjects could learn to adjust their reaction to the test inputs, so that SRE variations, and with that the variation in muscle activation, could be kept within bounds. With a reasonable number of practice runs, subjects could very well minimize their early reactions to the test inputs. Such adaptivity of reactions to test inputs was also reported elsewhere.[16]

Many muscle models suggest that the muscle behaviour is nonlinear.[13,23,24] For a linear muscle model such as the one used here, this would mean that one can find different estimates for the parameter values, depending on the working point in which the experiment was performed. In a three-element muscle model, one of the principal nonlinear effects would be that the damping constant of the CC increases with increased muscle activation. The other effect is a nonlinear force-length relation for the SEC, with a higher elasticity constant at higher stretch of the SEC.

To test the nonlinearity of the neuromuscular system, the experiments were performed at different offset moments. Prior to a test input, subjects were requested to exert a certain moment on the stick. The muscle activation needed to exert this moment should then be maintained, and kept constant, during the test input. In this manner the tests were performed at a range of different average activations

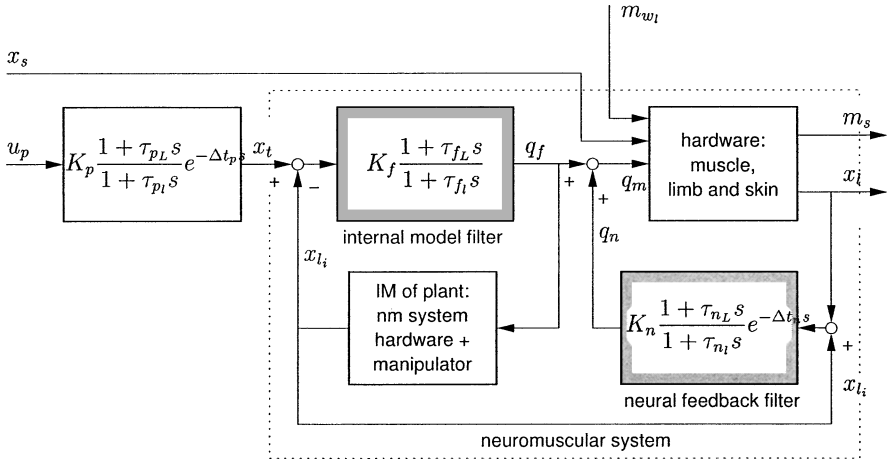

Fig. 3 Combination modeling pilot's control behavior and the neuromuscular system.

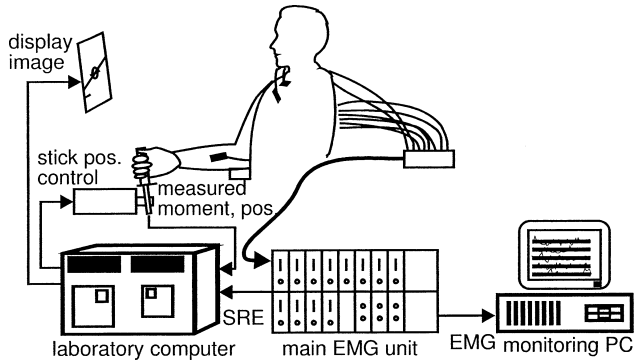

Fig. 4 Overview of the experimental setup.

of the muscles, and it could be expected, if nonlinear effects play a role in the envelope tested here, that the estimated parameters would consistently vary with the offset moment.

Equipment

The experiments were held in a small cabin in the laboratory for Stability and Control. Subjects were seated in a chair that was firmly mounted on a frame with the side stick. An overview of the equipment is given in Fig. 4.

The side stick is driven by an electrohydraulic motor, which permits the stick, also with the load of a subject's hand, to follow a position command signal from the laboratory computer with a bandwidth of approximately 50 Hz. Position of the stick and moment on the stick are measured and led through presample filters (second order, 200 Hz), before being digitized and read into the laboratory computer. The side stick is supplied with a handle, diameter 35 mm, with grooves for placement of the fingers. When a hand is correctly placed on the side stick, the center of the hand lies 90 mm above the stick rotation axis.

The subject's EMG signals on seven muscles were measured with a 12-channel EMG unit. These data were only used in the first experiment.

In front of the subjects, a small vector scan display (Tektronix 604, 100 mm wide, 125 mm high) was placed. The image on this display was generated with an analog computer and drawn with a refresh rate of 250 Hz. This image contained an aircraft symbol and an artificial horizon, a presentation with which all subjects, through their aeronautical background, were very familiar.

Test Input Description

In a single test of the experiment, the following phases can be distinguished:

1) The first phase is a run-in period, of 5 s, during which a mass-spring-damper system was simulated on the stick. The stick is movable, and the subject had the task of keeping it in the neutral position. For this he had to push against the stick with the offset force specified for this test. On a display in front of the subject, the deviation from the neutral position was shown. In the last second of the run-in period, the SRE signals were measured and averaged to obtain the base level SRE.

2) In the next 2.9 s the test signal, a preprogrammed change in stick position x_s, was applied. The test signal used in the experiment should not last too long because it would become very difficult for the subjects to keep their muscle activation constant over a longer period. The test signal should sufficiently excite the neuromuscular system so that parameter identification is possible, but the mechanical input should still be acceptable for subjects and not cause injuries. To provide a wide input spectrum, the test signal consisted of the sum of two sine-wave frequency sweeps (see the fourth plot in Fig. 5). One sweep started at 0.5 rad s^{-1} and ended at 18 rad s^{-1}, and the second sweep started at 150 rad s^{-1} going down to 15 rad s^{-1} (i.e., with decreasing frequency). The amplitude of the sweeps was determined by limiting the maximum stick position, speed, and acceleration to 0.279 rad, 6 rad s^{-1}, and 60 rad s^{-2}, respectively.

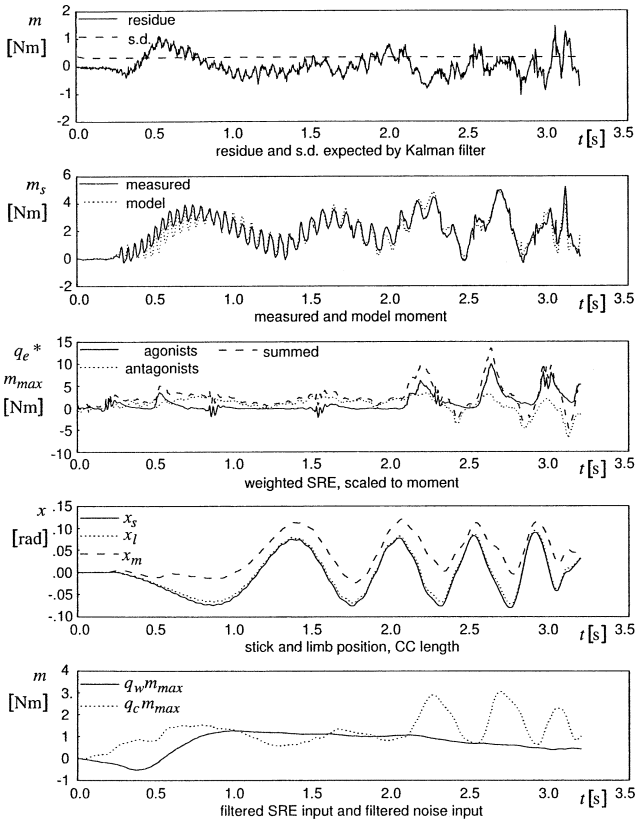

Fig. 5 Sample of the results produced by the estimation program, subject 3.

3) The tests were closed off with a run-out period, lasting 2.0 s. During this period, the same mass-spring-damper system that was used in the run-in period, with the same offset force, was simulated on the stick. The test signal ended with the stick in the neutral position, and if the subject had kept his muscle activation constant he should again exert the proper force to counter the offset force, leaving the arm and stick in equilibrium.

During the application of the test signal and the run-out period, an error measure was calculated based on the measured SRE. In time slices of 0.1 s, the SRE signals were averaged. At the end of a time slice, the difference between the averaged SRE and the base level SRE (measured in the second before the start of the test input) contributed to the error score. This score calculation used the SRE from the pectoralis major, sternal, and clavicular parts (medial rotation, i.e. pushing to the left) and the deltoid posterior, trapezius transversalis, and infraspinatus (lateral rotation). To further smoothen the presentation, the SRE error signal was filtered by a first-order low-pass filter with a time constant of 1s.

The SRE error signal was used to drive the error bar, on the left-hand side of the display (Fig. 4). Initially the error bar rests at the lower edge of the display, and then this bar rises with increasing error, a maximum deflection of the bar corresponded to a filtered error of 53 μV.

The experiments were performed at a range of 13 different offset moments. The maximum moment on the stick corresponded to a sideways force of 15 N. A positive force or moment on the stick is to the left. The minimum force, pushing to the right, was -12 N. The different moment levels were combined with two different test signals, the x_s signal of Fig. 5, and its mirror image. Each configuration was repeated five times, making a total of 130 tests. The tests were applied in a random order.

Data Processing and Estimation

Estimation Model

We attempted to estimate values of the parameters of the neuromuscular hardware. The neuromuscular hardware is a system with

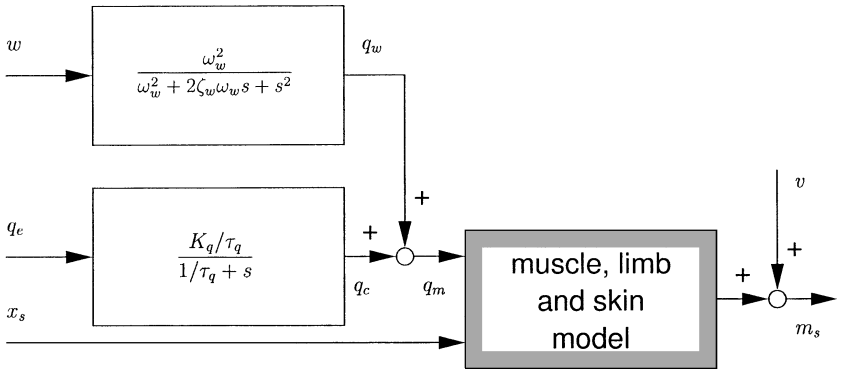

Fig. 6 Overview of the estimation model structure.

two inputs (Fig. 6), of which the side-stick position input is well known, and poses no particular problem for the estimation. Of the muscle activation q_m, only a rough indication can be obtained from the measured SRE signals.

By weighting and scaling the measured SRE signals,[17] an indication for muscle activation q_e. is obtained. To model the latency between muscle activation and the generation of muscle force, this signal is filtered with linear first-order lag, resulting in a contribution to the muscle activation q_c. This is a linear approximation of the processing proposed by Hof[24] and Winters and Stark.[13] To model the fact that the estimation of muscle activation is inaccurate, a second contribution to the muscle activation, q_w, is added. This signal is derived from a white-noise signal w and filtered with a second-order lag filter, with a bandwidth of $\omega_w = 1$ Hz and a damping of $\zeta_w = 0.75$. Remaining inaccuracies in the model and the measurement are modeled by a white noise v at the output of the muscle, limb, and skin model.

Summarizing, the combined estimation model has the following features (see Fig. 6):

1) The first feature is the neuromuscular system hardware model, with muscle activation input q_m, stick position input x_s, and the measured moment on the stick m_s as the output.

2) A white noise v, added to m_s to account for measurement noise is the second feature.

3) The next feature is a neural activation filter that translates the activation q_e estimated from the SRE signals into a muscle activation q_c. The time constant τ_q and a gain constant K_q are also included in the parameter estimation.

4) A white noise w, filtered by a second-order low-pass filter, to represent the unknown part of the muscle activation q_w is the last feature.

The identification method takes the noise at the system input w into account. It uses a Gauss–Newton search method to find the most likely, that is, maximum likelihood, values for the parameters.[25] This method uses a Kalman filter to supply the data for the likelihood function. As a side effect, the Kalman filter provides an estimate for the standard deviation of the difference between measured moment on the stick m_s and the model output (the residue). The intensity of the white noises w and v was adjusted so that the residue approximately matched its predicted standard deviation, resulting in intensities $W = 2$ Nm and $V = 0.1$ Nm for the standard deviation of noise w and v, respectively.

Data Processing

During the experiments, SRE data, stick position, and and the moment on the stick were recorded at a rate of 500 samples/s. The data used in the estimation started 0.2 s before the test input and include the full 2.9 s of the test input and an additional 0.1 s after the test input. For all signals the average of the first 0.2 s (with the stick–arm system in equilibrium) was calculated and subtracted from the recording, so that signals start at 0, simplifying the subsequent parameter estimation step.

Before each session with experiments, an EMG calibration experiment was run. The calibration coefficients from that experiment were used to obtain a muscle activation estimate q_e from five SRE signals. Because cross feed of heartbeat activity was present in some of these signals, a cardiac activity signal was also measured and used to eliminate this cross feed. The EMG calibration basically provides a best linear estimate for isometric force contraction based on SRE from these muscles. These calibration gains were used to form the activation signal q_e.

Each recording was individually used in the parameter estimation process. Because all tests were repeated five times, this resulted in five sets of parameter values for each of the 26 conditions. An example of the fit made by the parameter estimation program is given in Fig. 5.

The estimation of all parameter values of the linear model proved to be difficult. The muscle's series elastic spring constant K_e frequently attained unrealistically high values, in the order of 100 to 500 NM rad^{-1}.

To investigate the parameter estimation process, a computer simulation of the experiment was made, using the estimation model. Representative parameter values were chosen for the parameters of the model, and Gaussian input noises were used. The estimation process was repeated with the simulated data. From analysis of the Cramer–Rao lower bound, it appeared that the skin elasticity constant and the elasticity constant of the SEC could not be determined with the data from the experiment. The value K_e was fixed to $K_e = 30$ Nm rad^{-1}, based on data from Ref. 13 and the value of the elasticity constant for the skin model was fixed to a high value of $K_c = 300$ Nm rad^{-1}, so that skin model compression and extension would remain small enough to be realistic. The estimation was continued to obtain the remaining four parameters of the neuromuscular system model, B_m, I_a, K_{pec}, and B_c. The two parameters that controlled the use of the SRE-based estimate of the muscle activation signal, τ_q and K_q, were also varied in the parameter estimation process. Note that these two parameters do not characterize the neuromuscular system model and are therefore not included in the results.

During the parameter estimation, a considerable number of recordings produced one or more negative values for the parameters. For the parameters B_m, I_a, K_{pec}, B_c, and τ_q negative values are on physical grounds unacceptable. The recordings that produced negative values for one or more of these parameters were not further considered. Table 2 gives the resulting parameters, together with the standard deviation of the estimate (s.d. est. in Table 2) and the experimentally determined standard deviation (σ_{n-1} in Table 2), and the number of data sets that produced acceptable results, that is, positive spring constants, etc. The best results were obtained with the data from subject 3, where of the 130 data recordings 120 recordings produced acceptable results.

With the data from subject 3, it was investigated whether the offset moment has a systematic effect on the parameter values of the linear model, as is indicated by the properties of for example nonlinear model by Winters and Stark.[13] The parameter values for all recordings at a specific offset moment were averaged, and the results for the model parameters B_m, I_a, K_{pec}, and B_c are given in Fig. 7. A linear increase of the damping of the contractile component with

Table 2 Results of the parameter estimation of experiment 2

Subject	Result	B_m, Nm s/rad	K_{pec}, Nm/rad	B_c, Nm s/rad	I_a, kg m^2	K_e, Nm/rad	K_c, Nm/rad	K_q	τ_q, S
Subject 1	Mean	0.273	4.45	8.17	0.0539	30	300	0.256	0.465
$n=68$	σ_{n-1}	0.130	4.08	1.67	0.0074	——	——	0.104	0.171
	s.d. est.	0.017	0.28	0.20	0.0006	——	——	0.011	0.012
Subject 2	Mean	0.320	7.57	10.54	0.0656	30	3000	0.356	0.570
$n=56$	σ_{n-1}	0.153	5.48	1.46	0.0110	——	——	0.550	0.480
	s.d. est.	0.016	0.25	0.21	0.0007	——	——	0.047	0.035
Subject 3	Mean	0.538	9.14	7.01	0.0417	30	300	0.291	0.385
$n=120$	σ_{n-1}	0.241	5.39	1.14	0.0059	——	——	0.206	0.241
	s.d. est.	0.019	0.26	0.22	0.0006	——	——	0.029	0.019
Subject 4	Mean	0.292	8.67	13.56	0.0906	30	300	0.350	0.412
$n=73$	σ_{n-1}	0.167	7.79	1.43	0.0072	——	——	0.837	0.302
	s.d. est.	0.017	0.26	0.20	0.0007	——	——	0.116	0.039

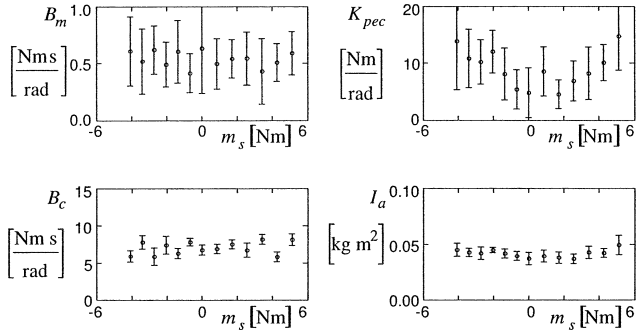

Fig. 7 Averages of estimated parameters of experiment 1, plotted against the offset force. Bars indicate $\pm 1\sigma$.

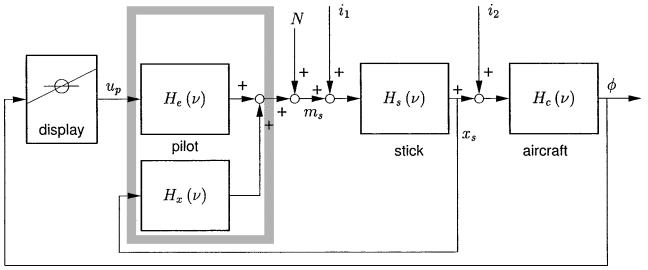

Fig. 8 Principle of the control task with two input signals. The shaded block corresponds to the model of Fig. 3.

increasing offset moment, which would have been expected on the basis of literature data, does not appear in the plot. Unexpectedly, a dependency of the muscle's parallel elasticity constant on the offset moment appears from the plot. The use of a nonlinear model of the neuromuscular system does not seem justified by this evidence.

Experiment II—Control Task

Experiment Principle

The second experiment described here is intended to test the properties of the neuromuscular system for subjects engaged in a continuous control task. Experiments with control tasks have been used extensively in the study of human control behavior (for example, see Refs. 5 and 26). Although it might not always be explicitly stated in the literature, in the analysis of these tasks the identified behavior is for the combination of the pilot, his neuromuscular system, the manipulator, and the display.

For conventional measurements of the pilot's control behavior, a disturbing signal is introduced to enable its identification. In this case, instead of one, two disturbing signals will be used: a conventional signal that is introduced at the input of the controlled system, i_2, and a second signal that has the effect of a disturbing moment on the side stick, i_1 (see Fig. 8).

Using the two disturbing signals, and assuming linear superposition of the reaction to these signals, two parts of the pilot's control behavior can be identified (see Fig. 8). These parts are 1) $H_e(\nu)$, the moment exerted on the stick in response to the error perceived on the display, and 2) $H_x(\nu)$, the moment exerted on the stick in response to the movement of the stick.

Table 3 Properties of the three sticks used in the experiment (the mass, spring, and damping constants are defined at 90 mm above the stick rotation axis)

Stick no.	Description	Mass, kg	Spring constant, Nm^{-1}	Damping, N s m^{-1}
1	Standard	1.5	400.0	26.1
2	No spring	1.5	0.0	26.1
3	High mass	4.0	400.0	26.1

These transfer functions use the variable $\nu = j\omega$ instead of the Laplace variable s to express the fact that they are expressions for pilot behavior in continuous control tasks only. These two parts of the pilot's behavior can also be generated by the model described in Sec. Model. The identification of the measured data results in describing frequency-response functions for $H_e(\nu)$ and $H_x(\nu)$. Using these as intermediate results, and using the parameters for the hardware determined with experiment 2, an attempt was made at estimating the remaining parameters of the model for the neuromuscular system.

Experiment Description

To test the model and obtain a representative set of parameter values, a second experiment was performed, in which four subjects, all qualified airline pilots, participated. The equipment used is the same as for experiment I.

Subjects used a side stick to control a linear system that represents the roll properties of an aircraft. The system contains an integrator and a roll time constant of 0.5 s. The Laplace representation of the controlled system is

$$H_c(s) = K_a/s(1 + \tau_a s) \tag{1}$$

The gain of the controlled system is $K_a = 2$ rad/rad; the roll time constant is $\tau_a = 0.5$ s. This roll time constant makes the system relatively fast and therefore not too difficult to control. (The roll dynamics are in the order of those of a Fokker F27 at approach speed.)

The position of the side stick is used for the control input of the controlled system. The output of the system, representing the roll angle of an aircraft, is presented on the horizon display generated on the analog cathode ray tube (CRT).

Passive side-stick dynamics were simulated on the servocontrolled side stick. This simulation resulted in a side stick with linear dynamics, with a stick mass M_s, a linear damping constant B_s, and a spring constant K_s, defined defined for a point at 90 mm above the stick's rotation axis. To investigate whether a change in stick properties would affect the behavior of the neuromuscular system, three different stick dynamics were used (see Table 3). The maximum excursions are 22 deg to the left and right, from the neutral

Table 4 Sine function components of the two disturbing functions: frequency of sine waves, initial phase angle and amplitude of the individual sine waves

Disturbing function i_1, side-stick input				Disturbing function i_2, contr. system input			
Number of waves f_{1_j}	Frequency ν_{1_j}, Hz	In phase ϕ_{1_j}, rad	Amplitude A_{1_j}, N	Number of waves f_{2_j}	Frequency ν_{2_j}, Hz	In. phase ϕ_{2_j}, rad	Amplitude A_{2_j}, deg
6	0.0732	1.3758	0.6995	5	0.0610	2.6231	1.5245
14	0.1709	0.2956	0.6975	13	0.1587	4.3151	1.6538
23	0.2808	4.2654	0.6932	22	0.2686	3.7006	1.8813
38	0.4639	4.2681	0.6819	37	0.4517	5.8461	2.2539
53	0.6470	5.8728	0.6660	51	0.6226	5.3166	2.4156
73	0.8911	2.4096	0.6394	71	0.8667	3.3108	2.3154
103	1.2573	3.2636	0.5926	101	1.2329	0.5778	1.9152
139	1.6968	5.2211	0.5338	137	1.6723	4.1087	1.5026
194	2.3682	0.2172	0.4517	193	2.3560	2.6138	1.0991
227	2.7710	0.3359	0.4097	226	2.7588	4.4057	0.9453
263	3.2104	3.3282	0.3701	262	3.1982	5.7197	0.8192
313	3.8208	4.2170	0.3246	311	3.7964	4.7890	0.6926
383	4.6753	0.0484	0.2753	382	4.6631	1.6490	0.5655
458	5.5908	2.4091	0.2358	457	5.5786	0.2982	0.4735
547	6.6772	0.4200	0.2009	546	6.6650	4.6249	0.3967

position. During the experimental runs, these maximum positions were never reached. The use of the servocontrolled stick allows the addition of the test signal i_1 as a disturbing moment on the stick.

The duration of an experimental run is approximately 97 s. The first 15 s is used as run-in time during which the subject has the opportunity to adjust himself to his task. The following 81.92 s is recorded with a sample frequency of 50 Hz, resulting in 4096 points of data. The simulation of the system dynamics and the side-stick dynamics is performed at a sample frequency of 500 Hz.

The two test signals each consisted of the sum of 15 sine signals. The use of such a test signal allows a determination of the bias and variance of the estimated frequency responses.[17,27,28] The signal must however appear completely random to the subjects; an awkward choice of the sine frequencies would allow subjects to recognize a repeating pattern in the test signal. Furthermore, it is essential for the estimation that each component of the test signal has an integer number of periods in the measurement window. The frequencies for the sine components are thus an integer multiple of the base frequency $2\pi/81.92$ rad s^{-1}, and none of the sines is an integer multiple of other sine components, preventing recognition of harmonic components. The bandwidth of the test signals is limited by using the magnitude of a first-order system, with a cutoff frequency of 4π for test signal 1, and of a second-order system, with a corner frequency of $\omega = 3/4\pi$, and compensated for the roll time constant of the controlled system, for test signal 2 (see Table 4).

Data Processing

Data processing of the experimental results is performed in three different steps:

1) The recorded data (moment on the stick, stick position, and displayed error) is averaged over all runs with the same configuration. This is possible because for each experimental configuration the subjects performed eight runs with the same test signals. Averaging the recorded data improves the signal-to-noise ratio of the data.

2) The data are analyzed in the frequency domain. This results in describing functions in this domain, describing gain and phase lag of H_x and H_e at the test signal frequencies, and in bias and variance of these estimates.

3) The describing functions and their statistical properties are then used to estimate the parameters of the model of the pilot and the neuromuscular system.

The nonparametric estimation step results in separate describing functions for the pilot's response to stick movement and to the error presented on the display. We want to use these describing functions to estimate the parameters in the model. The parameters estimated with the first experiment all describe the physical hardware of the neuromuscular system. It is assumed that these parameters are also valid for the second experiment, and the estimation procedure will concentrate on estimating parameters for the following model parts: 1) the internal model filter, K_f, τ_{f_l}, and τ_{f_L}; 2) the neural feedback, K_n, τ_{n_l}, τ_{n_L}, and Δt_n; and 3) the pilot's control behavior, K_p, $\tau_{\mathrm{p_l}}$, $\tau_{\mathrm{p_L}}$, and Δt_p.

It is well known that pilots adapt their control behavior to the controlled task.[5] That means that the values for the parameters K_p, $\tau_{\mathrm{p_l}}$, $\tau_{\mathrm{p_L}}$, and to a somewhat lesser extent Δt_p, will depend on the configuration of the controlled system. The same very probably goes for adaptation to the manipulator; and thus the parameter values of the internal model filter and possibly the neural feedback can be expected to vary depending on the manipulator configuration.[15,16,20] This means that any parameter values found in the estimation process are not necessarily valid for side sticks or other manipulators with different characteristics than the ones chosen here, nor for other control tasks.

A generic minimization procedure, based on a Gauss–Newton calculation, is used to obtain a best fit of the transfer functions of the neuromuscular system model transfer functions $\tilde{H}_e$ and $\tilde{H}_x$ to the measured points of the describing functions. Because the variance of the estimate for the describing functions is known, the estimate of the parameters can use a weighted criterion:

$$
\begin{aligned}
J = \sum_{j=1}^{j=15} \Bigg\{ & \frac{1}{\mathrm{var}\left[\hat{H}_e\left(\nu_{1_j}\right)\right]} \left|\hat{H}_e\left(\nu_{1_j}\right) - \tilde{H}_e\left(\nu_{1_j}\right)\right|^2 \\
& + \frac{1}{\mathrm{var}\left[\hat{H}_e\left(\nu_{2_j}\right)\right]} \left|\hat{H}_e\left(\nu_{2_j}\right) - \tilde{H}_e\left(\nu_{2_j}\right)\right|^2 \Bigg\} \\
& + \sum_{j=1}^{j=15} \Bigg\{ \frac{1}{\mathrm{var}\left[\hat{H}_x\left(\nu_{1_j}\right)\right]} \left|\hat{H}_x\left(\nu_{1_j}\right) - \tilde{H}_x\left(\nu_{1_j}\right)\right|^2 \\
& + \frac{1}{\mathrm{var}\left[\hat{H}_x\left(\nu_{2_j}\right)\right]} \left|\hat{H}_x\left(\nu_{2_j}\right) - \tilde{H}_x\left(\nu_{2_j}\right)\right|^2 \Bigg\}
\end{aligned} \tag{2}
$$

The data obtained from the nonparametric identification step $H_x(\nu)$ and $H_e\nu$ is used at all frequencies of the conventional test signal i_2, indices 2_j, and at the frequencies of the test signal on the side stick i_1, indices 1_j. After the parameter estimation procedure it is also checked whether the combination of the pilot model, neuromuscular system, and aircraft model is stable with the newly found parameters.

Table 5 Parameter values for the neuromuscular system model (parameters for the neuromuscular system hardware can be found in Table 2)

	Subject 2			Subject 3			Subject 4		
Parameter	st. 1	st. 2	st. 3	st. 1	st. 2	st. 3	st. 1	st. 2	st. 3
K_p	0.707	0.256	0.437	0.520	0.274	0.489	0.946	0.769	0.689
Δt_p, s	0.247	0.309	0.213	0.212	0.285	0.270	0.267	0.259	0.247
K_n, rad^{-1}	1.200	1.287	1.591	3.187	1.345	1.259	1.425	5.443	1.704
τ_{n_L}, s	0.1[a]	0.1[a]	0.07[a]	0.1[a]	0.1[a]	0.2[a]	0.1[a]	0.1[a]	0.08[a]
τ_{n_l}, s	0.491	0.119	0.427	0.477	0.104	0.273	0.138	0.312	0.056
Δt_n, s	0.02[a]	0.02[a]	0.02[a]	0.02[a]	0.02[a]	0.02[a]	0.02[a]	0.02[a]	0.02[a]
K_f, rad^{-1}	1.546	3.309	6.521	2.952	3.199	1.566	2.969	7.846	6.612
τ_{f_L}, s	0.0[a]	0.1[a]	0.0[a]	0.0[a]	0.1[a]	0.1[a]	0.08[a]	0.1[a]	0.1[a]
τ_{f_l}, s	0.3[a]	0.5[a]	1.0[a]	0.3[a]	0.4[a]	0.3[a]	0.3[a]	0.5[a]	0.5[a]

[a]Obtained through manual parameter adjustment.

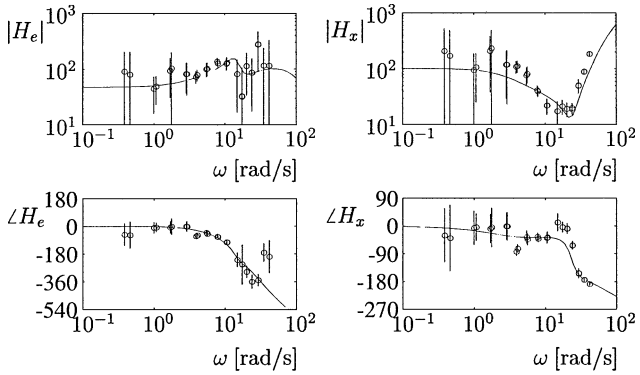

Fig. 9 Results of the nonparametric estimation of H_e and H_x, subject 3, stick 1.

Results

As an example, the results from the nonparametric estimation are given in Fig. 9, which shows the estimated describing functions, with lines indicating the standard deviation of the estimate. For the frequencies above 2 rad s^{-1}, the standard deviation of the $\hat{H}_x$ estimate is fairly small. For frequencies of 2.84 rad s^{-1} and higher, thus from the fourth estimated pair of points and onward in Fig. 9, the biases in the estimated points of the describing functions were smaller than 1% and could be neglected. The biases in the first three pairs of estimated points were often considerable, in the order of 30 to 100% of the sizes of $\hat{H}_e$ and $\hat{H}_x$.

For subjects 2, 3, and 4 the standard deviation of the estimates was acceptable; the estimate of the describing function of subject 1 was considerably worse. It appeared that the intensity of the noise injected by this subject was approximately 10 times larger than what was found with the other subjects. This did not severely affect the subject's control performance, but it had an adverse effect on the estimation of the describing functions. For the following fit of the parametric model to the describing functions, the data from this subject were excluded.

At high frequencies, above 10 rad s^{-1}, the standard deviation of $\hat{H}_e$ is very large. Normally these frequencies are not measured in a closed-loop control task because the human operator cannot display a consistent control behavior at these frequencies. In this task these frequencies were included because the behavior of H_x is of interest at these frequencies. The standard deviation of $\hat{H}_x$ in this region is acceptable because for this response no conscious control actions are necessary; only the neuromuscular system hardware and the neural feedback play a role.

The moment response to the stick movement $\hat{H}_x$ is in most cases fairly level at lower frequencies (1–5 rad s^{-1}), as can be seen in Fig. 9. The amplitude of the response to stick movement $|\hat{H}_x|$ is in the order of 50 to 100 Nm rad^{-1}. This is an order of magnitude larger than the stiffness of the parallel elastic component of the muscles as found with experiment 2. It appears that by neural feedback the subjects maintain a relatively high stiffness of the neuromuscular system.

Between 10 and 20 rad s^{-1} there is a dip in the magnitude of $\hat{H}_x$. At frequencies below this dip, the response to the stick position is dominated by the neural feedback and the passive elasticity of the muscle. For frequencies above this dip, the response to the stick position is dominated by the inertia of the arm. At these frequencies, above 20 rad s^{-1}, the slope of the describing function is +2 on a log-log scale, corresponding to the response of the arm mass to the movement of the stick.

There is no clear influence of the stick properties on the describing functions $\hat{H}_e$ and $\hat{H}_x$. Also for the different subjects these functions are similar. For example, for subject 4, describing function $\hat{H}_e$ has a somewhat higher gain than for the other subjects. With the describing functions estimated for subjects 2–4, the parameters of the model were determined. First the parameters were adjusted manually, until a good fit between the describing functions $\hat{H}_e$ and $\hat{H}_x$. and their model equivalents was found. Subsequently this fit was further improved, using a Gauss–Newton search that minimized the criterion of Eq. (2).

The results are given in Table 5. Not all parameters could be found with the parameter estimation procedure. Combinations of the lead time constant τ_{n_L}, lag time constant τ_{n_l}, and time delay Δt_n of the neural feedback model were highly correlated and the estimation produced large standard deviations for these parameters. The lead and lag time constant of the filter for the internal model τ_{f_L} and τ_{f_l} were also highly correlated. Therefore a selection had to be made for the parameters that were further updated with the iterative least-squares method. It appeared that a maximum of five parameters could be estimated. These were the gain of the pilot equalization K_p, the pilot's time delay Δt_p, the gain of the neural feedback K_n, the lag time constant of the neural feedback τ_{n_l}, and the gain of the filter for the internal representation K_f. The values found with the manual adjustment were inserted for the six parameters that were not further updated with the least-squares estimation.

Conclusions

The present paper shows the development of a model for the neuromuscular system and two experiments with a (fixed-base) control loaded side stick to obtain parameter values for the model.

The first experiment is directed at obtaining parameters for the hardware of the neuromuscular system. It proved to be possible to obtain four of this part's parameters, namely, limb inertia, contractile component damping, skin damping, and parallel component elasticity. Series component elasticity and skin model elasticity needed to be set to fixed values. A seventh parameter, the contractile force corresponding to maximum muscle activation, is not observable from the experiment. It can be set to any reasonable value, because it only serves as a redundant gain constant. Nonlinear effects with the limited range of forces typical in normal control actions were only observed in the parallel elastic component.

Possibly the model order might be reduced further, by omitting the series elastic component. This could however affect model behavior at high frequencies.

The second experiment tested the neuromuscular system in a closed-loop control task, with two test signals. Application of

nonparametric estimation techniques task provides two describing functions for pilot behavior, one for the response to an error perceived on a display and the other for the response to movement of the stick. Using these data and using the parameter values for the neuromuscular system from the first previous experiment, it is possible to estimate five of the 11 parameters that describe the pilot's control behavior and the control and feedback loops of his neuromuscular system.

Inspection of the subjects' describing functions for force response to the stick movement reveals that the neuromuscular reflexes are capable of increasing the effective stiffness of the limb to levels of 50 to 100 $\mathrm{Nm\,rad^{-1}}$. However *unlike many well-designed control loops, including models of manual control*, the neuromuscular reflex loop does not exhibit integrating open-loop behavior, the neuromuscular system seems to be limited to proportional and possibly derivative control, and the model could be simplified by removing the lag term in the neuromuscular feedback loop.

The three different stick properties chosen in this experiment do not lead to significantly different behavior from the subjects. In hindsight, this is not surprising. A high stiffness maintained by the neuromuscular system leads for all three sticks to the best suppression of the disturbing signal and to the highest-bandwidth response of the combined stick and neuromuscular system. A task requiring a different adaptation (e.g., a force task, in which exerted force needs to be held constant) could induce different settings of the neural feedback.

Further investigation into the nature of the adaptation of the neuromuscular system system to the tasks demands is needed. The limits of the adaptation of the neural feedback, and those of the control signal generation with the internal representation need to be explored further, in experiments with different stick dynamics and also different task settings.

References

[1]Hoh, R. H. E., "Proposed Mil. Standard and Handbook,—Flying Qualities of Air Vehicles," USAF, Tech. Rept. AFWAL-TR-82-3081, Nov. 1982.

[2]Johnston, D. E., and Aponso, B. L., "Design Considerations of Manipulator and Feel System Characteristics in Roll Tracking," NASA, CR-4111, 1988.

[3]Hosman, R. J. A. W., and van der Vaart, J. C., "Active and Passive Side Stick Controllers: Tracking Task Performance and Pilot Control Behaviour," *AGARD Conference Proceedings 425*, NATO, AGARD, Brussels, 1988, pp. 26-1–26-11.

[4]Morris, A., and Repperger, D. W., "Discriminant Analysis of Changes in Human Muscle Function When Interacting with an Assistive Aid," *IEEE Transactions on Biomedical Engineering*, Vol. 35, No. 5, 1988, pp. 316–322.

[5]McRuer, D. T., and Jex, H. R., "A Review of Quasi-Linear Pilot Models," *IEEE Transactions on Human Factors in Electronics*, Vol. 8, No. 3, 1967, pp. 231–249.

[6]Kleinman, D. L., Baron, S., and Levison, W. H., "An Optimal Control Model of Human Response Part I: Theory and Validation," *Automatica*, Vol. 6, No. 3, 1970, pp. 357–369.

[7]Jex, H. R., "Problems in Modeling Man-Machine Control Behavior in Biodynamic Environments," *Proceedings of the 7th Annual Conference on Manual Control*, NASA, Ames, 1971, pp. 3–13.

[8]Hess, R. A., "Model-Based Investigation of Manipulator Characteristics and Pilot/Vehicle Performance, *Journal of Guidance, Control, and Dynamics*, Vol. 6, No. 5, 1983, pp. 348–354.

[9]Hess, R. A., "Theory for Roll-Ratchet Phenomenon in High-Performance Aircraft," *Journal of Guidance, Control, and Dynamics*, Vol. 21, No. 1, 1998, pp. 101–108.

[10]Allen, R., Jex, H., and Magdaleno, R., "Manual Control Performance and Dynamic Response During Sinusoidal Vibration," Systems Technology, Inc., Tech. Rept. STI TR-1013-2, USC, Los Angeles, June 1973.

[11]Höhne, G., "Roll Ratcheting: Caus and Analysis," Ph.D. Dissertation, Institut für Flugsystemtechnik Braunschweig, Technische Univ., Braunschweig, Braunschweig, Germany, 2001.

[12]Koehler, R., "A Unified Approach for Roll Ratcheting Analysis," *Journal of Guidance, Control, and Dynamics*, Vol. 22, No. 5, 1999, pp. 718, 719.

[13]Winters, J. M., and Stark, L. W., "Analysis of Fundamental Human Movement Patterns Through the Use of In-Depth Antagonistic Muscle Models," *IEEE Transactions on Biomedical Engineering*, Vol. 32, No. 10, 1985, pp. 826–837.

[14]Hof, A. L., and Berg, J. W. V. D., "EMG to Force Processing I: An Electrical Analogue of the Hill Muscle Model," *Journal of Biomechanics*, Vol. 14, No. 11, 1981, pp. 747–758.

[15]Happee, R., "Adaptation of Unexpected Variations of an Inertial Load in Goal Directed Movements," *Proceedings of the 5th IFAC Congress on the Analysis, Design and Evaluation of Man-Machine Systems*, IFAC, Laxenburg, Austria, 1992.

[16]Nashner, L. M., and Meiry, J. L., "Sensory Feedback in Human Posture Control," *Proceedings of the 6th Annual Conference on Manual Control*, Wright Patterson Air Force Base, Dayton, OH, April 1970, pp. 249–268.

[17]van Paassen, M. M., "Biophysics in Aircraft Control—a Model of the Neuromuscular System of the Pilot's Arm," Ph.D. Dissertation, Faculty of Aerospace Engineering, Delft Univ. of Technology, Delft, The Netherlands, June 1994.

[18]van Paassen, M. M., "Measurements of the Neuromuscular System Using Test Inputs Generated by the Electro-Hydraulic Side Stick Controller," Master's Thesis, Technical Univ. Delft, Faculty of Aerospace Engineering, The Netherlands, June 1988.

[19]van Paassen, M. M., "Modelling the Neuromuscular System for Manual Control," *Proceedings of the 9th European Annual Conference on Human Decision Making and Manual Control*, JRC Ispra, Ispra, Sept. 1990.

[20]Schmidt, R. A., "A Schema Theory of Discrete Motor Skill Learning," *Psychological Review*, Vol. 82, No. 4, 1975, pp. 225–260.

[21]Hof, A. L., and Berg, J. W. V. D., "EMG to Force Processing II: Estimation of Parameters of the Hill Muscle Model for the Human Triceps Surae by Means of a Calfergometer," *Journal of Biomechanics*, Vol. 14, No. 11, 1981, pp. 759–770.

[22]Hof, A. L., and Berg, J. W. V. D., "EMG to Force Processing III: Estimation of Model Parameters for the Human Triceps Surae Muscle and Assessment of the Accuracy by Means of a Torque Plate," *Journal of Biomechanics*, Vol. 14, No. 11, 1981, pp. 771–785.

[23]Huxley, A. F., "Muscle Structure and Theories of Contraction," *Progress in Biophysics and Biophysical Chemistry*, Vol. 7, No. 7, 1957, pp. 257–318.

[24]Hof, A. L., "EMG and Muscle Force: an Introduction," *Human Movement Science 3*, Elsevier, Amsterdam, 1984, pp. 119–153.

[25]Loos, P. J. G., "Maximum Likelihood Parameter Estimation for Stochastic Systems," Master's Thesis, Faculty of Aerospace Engineering, Delft Univ. of Technology, The Netherlands, Jan. 1988.

[26]van der Vaart, J. C., "Modelling of Perception and Action in Compensatory Manual Control Tasks," Ph.D. Dissertation, Faculty of Aerospace Engineering, Delft Univ. of Technology, The Netherlands, Dec. 1992.

[27]van Paassen, M. M., "Human Operator Response to Visual and Proprioceptive Inputs in a Control Task with a Side Stick," *Proceedings of the 10th European Annual Conference on Human Decision Making and Manual Control*, Univ. of Liege, Liege, Belgium, Nov. 1991.

[28]van Paassen, M. M., and Mulder, M., "Identification of Human Operator Control Behaviour in Multiple-Loop Tracking Tasks," *Proceedings of the 7th IFAC/IFIP/IFORS/IEA Symposium on Analysis, Design and Evaluation of Man-Machine Systems*, IFAC, Laxenburg, Austria, 1998.